

# Radio Frequency Interference Survey Over the 1.0–10.4 GHz Frequency Range at the Goldstone-Venus Development Station

S. Gulkis and E. T. Olsen  
Space Physics and Astrophysics Section

M. J. Klein and E. B. Jackson  
Telecommunications and Data Acquisition Science Office

*The results of a low sensitivity Radio Frequency Interference (RFI) survey carried out at the Venus Station of the Goldstone Communications Complex are reported. The data cover the spectral range from 1 GHz to 10.4 GHz with a 10-kHz instantaneous bandwidth. Frequency and power levels were observed using a sweep-frequency spectrum analyzer connected to a 1-m diameter antenna pointed at zenith. The survey was conducted from February 16, 1987 through February 24, 1987.*

## I. Introduction

Plans are currently being made at the Jet Propulsion Laboratory to carry out a comprehensive, all-sky search for radio signals of extraterrestrial origin. The Search for Extraterrestrial Intelligence (SETI) survey will employ the Goldstone Communication Complex near Barstow, California and other sites in the northern and southern hemispheres. The principal parameters of this survey are given in Table 1. In preparation for this search, JPL has constructed a radio spectrum surveillance system (RSSS) and made a series of measurements of the RFI environment at the Goldstone-Venus development station. Described in this article are the receiving system used [1], and the results of one low-sensitivity survey performed February 16–24, 1987. Additional surveys in restricted frequency bands and with higher sensitivity have been carried out in the interim. These surveys have not been fully analyzed at this time. This RFI survey effort is expected to continue for

several more years. Efforts will be concentrated on establishing trends and on attaining sensitivity commensurate with levels that will be achieved by SETI.

## II. The Radio Spectrum Surveillance System

The RSSS used for the observations reported here consisted of a log-periodic feed, a 1-meter parabolic antenna, a set of seven GaAs FET amplifiers (followed by transistor amplifiers) covering the spectrum from 1.0–10.4 GHz, and a Tektronix 494P swept spectrum analyzer. Figure 1 shows a block diagram of the receiving system. A Tektronix 4052A digital computer/controller automatically controls the antenna azimuth, noise diode, amplifier section, spectrum analyzer, and dual-floppy disk recorder. The spectral data are processed in the 4052A in near real time to determine whether a specified power threshold has been exceeded anywhere in the

spectrum. The data describing such events are written on the floppy disks at the field station for further off-line analysis at JPL.

The antenna and amplifiers are mounted atop the roof of a mobile trailer van. The spectrum analyzer, computer, and recording equipment are mounted in a rack inside the van. For the observations reported here, the van was parked at the Goldstone-Venus development station (DSS 13), about 30 meters south-west of the main control building. In this location, the van is approximately 150 meters east of the 26-meter antenna. Figure 2 shows a photograph of the site to illustrate the relative positions of the control building, the 26-meter antenna, and the RSSS.

Data recorded on the floppy disks are taken to JPL and copied onto a hard disk of a VAX 11/750 computer for further analysis. A commercially available database program, INGRES, is used to retrieve the data; custom software is used in conjunction with INGRES to perform parameter searches and generate various graphical displays.

### III. Observations

The observations were carried out in a fully automated mode by pre-scheduling the controller to scan the spectrum analyzer from 1.0 GHz to 10.4 GHz repeatedly at a resolution bandwidth of 10 kHz. The time required to complete a single-frequency scan was 40 minutes, and in total, 232 scans were made over the course of the survey. In order to expedite the survey, the antenna main beam remained motionless and pointed in the direction of the zenith instead of scanning the horizon. In the zenith orientation, the antenna gain resembles that of an omnidirectional antenna for radiation that arrives along the horizon. Assuming that the antenna gain in the direction of the horizon is the same as that from an omnidirectional antenna, the effective area for the survey is approximately  $0.1 \times \lambda^2$ , where  $\lambda$  is the wavelength of the observation. The effective area for on-axis signals is approximately  $0.5 \text{ m}^2$ . Power levels reported in this article assume an omnidirectional antenna.

Each frequency was observed a total of 232 times, with nearly uniform coverage with time of day. Figure 3 shows the distribution of observations ("looks") with day of the week. Each day of the week is further divided into six 4-hour intervals starting at midnight. The weekdays Monday and Tuesday were observed most frequently because the survey began on a Monday and extended for nearly nine contiguous days. Sunday was observed least frequently because of an interruption due to a full storage disk. Only the first 4-hour interval (midnight to 4:00 a.m.) was observed on Sunday. A system noise temperature calibration was automatically performed daily

between 3:00 a.m. and 4:00 a.m. local time. Table 2 gives the parameters used in the survey.

### IV. Results

A total of 37,589 events were detected in the survey. Figure 4 shows a histogram of the number of events exceeding the threshold as a function of received power level. Note that the power levels for some interfering signals exceeded  $-90 \text{ dBm}$ . These signals were traceable to local microwave transmitters. The relatively low number of signals detected with power levels less than  $-118 \text{ dBm}$  is believed to be caused by the non-uniform sensitivity of the survey which varied by approximately 7 dBm from one end of the band to the other due to increasing receiver noise temperature at higher frequencies. It has not been concluded that weaker signals are less prevalent than stronger signals; further work is planned to clarify the situation at lower power levels. Figure 5 shows the cumulative distribution of events as a function of minimum received power level.

Figure 6 shows the probability of a signal exceeding the threshold as a function of frequency over the full frequency range of the survey, 1.0–10.4 GHz. The frequency resolution of the graph is approximately 10 MHz. This figure reveals that the probability is very nonuniform across the survey frequency range. The highest incidence of interference is in two frequency ranges: 1.0–3.0 GHz and 7.7–8.3 GHz. Figure 7 shows an enlargement of Fig. 6 in the frequency range 1.0–2.0 GHz. The frequency resolution of Fig. 7 is approximately 1 MHz. It can be seen from this figure that the "Water Hole" frequency range, 1.4–1.7 GHz, contains a significant amount of interference, but that the radio astronomy bands near 1.4 GHz and 1.6 GHz are relatively quiet, at least at the sensitivity achieved by this particular survey.

Figure 8 displays the probability of RFI events over the full 1.0–10.4 GHz range as a function of day of week. As in Fig. 3, each day is divided into six 4-hour intervals. Note that no observations were made between 0400 UT Sunday and 0400 UT Monday, which explains the lack of events during this time interval. This figure illustrates the pervasive nature of the interference. RFI events were observed every day of the week, with little change in probability of occurrence with time of day.

Table 3 provides a list of the frequencies and approximate frequency ranges that have exhibited an interfering signal at least 10 percent of the time they were observed. A worst-case estimate of the fraction of the observed band which is obscured by RFI can be made by adding up all the frequency ranges in Table 3. From this crude summation, it is found that 7.21 MHz, or approximately 7.7 percent of the 9.4-GHz survey bandwidth is affected by RFI at least 10 percent of the time.

A more detailed analysis of the raw data, examining each channel individually rather than in the frequency ranges indicated in Table 3, is shown in Fig. 9. This figure depicts the percent of the observed band obscured by RFI at least 10 percent of the time as a function of a limiting received power. The solid curve spanning the range from -100 dBm to -116 dBm is derived from the survey. Since the sensitivity level at which SETI will be operating is close to -170 dBm, it is of great interest to determine experimentally the shape of this curve at lower power levels. The dashed curves shown in Fig. 9 are crude extrapolations to lower power levels.

Several statistical models which might be helpful in providing a basis for understanding the present and future RFI survey results were considered. In the first model it was assumed that the effective isotropic radiated power (EIRP) of each transmitter is identical, that the transmitters are randomly distributed in area, and that the transmitter frequencies are randomly distributed. These assumptions are certainly incorrect since (1) transmitter frequency allocations are not random, (2) transmitter positions are generally clustered, and (3) EIRPs are not constant. Nevertheless, the model describes the extreme situation of extrapolating the local environment at Goldstone to more distant regions, assuming the areal density of transmitters is constant. For this model, the fraction of the survey band obscured,  $f$ , as a function of the received power,  $P$ , is given by the expression:

$$f = 1 - e^{-\frac{k}{P}} \quad (1)$$

where  $k$  is a constant. The constant,  $k$ , is a function of the areal density of transmitters, the fractional bandwidth covered by each transmitter, the EIRP of each transmitter, and the collection area of the receiving system. The dashed curve in Fig. 9 shows a graph of this equation with  $k$  taken to be -136.7 dBm (note: convert power from dBm to Watts when using the equation). This equation thus predicts that 63 percent of the band is obscured at the -136.7-dBm level. Preliminary results of a subsequent survey, not reported here, show that the interference is much less than this model predicts. The spatial distribution could just as well have been ignored in this model, and the spectral power density assumed to arrive at the same result. In reality, some combination of areal density and spectral power distribution are needed for a complete description.

A simple estimate of a lower bound for this model can be made by assuming that the areal density of transmitters goes

abruptly to zero at some arbitrary radius. This condition might exist if the detectable transmitters were clustered near Goldstone, or if distant transmitters were obscured by the horizon. This lower bound model can be expressed by the pair of equations:

$$\begin{aligned} f &= 1 - e^{-\frac{k}{P}} & P \geq P_m \\ f &= 1 - e^{-\frac{k}{P_m}} & P \leq P_m \end{aligned} \quad (2)$$

The locus of points defined by these equations is shown by the two dotted lines in Fig. 9. Each assumes the same value of  $k$  as above but different minimum power cutoffs. One is drawn for a value of  $P_m = -125$  dBm, and the other for a value of  $P_m = -114$  dBm.

It is impossible to draw any firm conclusions about these models until more sensitive survey data are available. The models are highly simplified and do not consider the reality of more than one population of transmitters. For example, the sensitivity of this survey was too low to detect signals from geosynchronous satellites. We emphasize that any attempt to extrapolate these data to the power levels of interest to SETI is considered to be highly uncertain because of the more than 50-dBm power level difference between the experimental data and the SETI power regime.

## V. Conclusions

It is concluded from this low-sensitivity, broad-band survey that most of the strong ( $> -116$  dBm) RFI in the 1-10 GHz band occurs in relatively few bands. Nearly 1 percent of the entire band shows interference at the -116-dBm level or stronger with a probability of occurrence  $\geq 10$  percent. The interfering signals do not appear to show a strong dependence on time of day or on day of the week. Interfering signals from satellites will probably show up at power levels significantly less than were achieved in this survey. Surveys at approximately 30 dB better sensitivity can be achieved with the current RSSS in a reasonable time through (1) use of a discone antenna to provide higher sensitivity along the horizon, and (2) observing with a more narrow bandwidth. Observations are currently being made with higher sensitivity using both of these techniques. Surveys at even greater sensitivity, approaching those achieved by SETI in the sidelobes, must await more sensitive systems.

## Reference

- [1] B. Crow, A. Lokshin, M. Marina, and L. Ching, "SETI Radio Surveillance System," *TDA Progress Report 42-82*, vol. April-June 1985, Jet Propulsion Laboratory, Pasadena, California, pp. 173-184, August 15, 1985.

**Table 1. All-sky survey parameters**

Spatial coverage	Entire celestial sphere
Frequency range	1-10 GHz inclusive and higher frequency spot bands
Duration	≈ 6 years
Frequency resolution	≈ 30 Hz
Instantaneous bandpass	≈ 250 MHz
Sensitivity	$\leq 10^{-23} \sqrt{\nu_{\text{GHz}}} \text{ Wm}^{-2}$
Polarization	Simultaneous dual circular
Signals	Primarily CW with natural radio astronomy fallout

**Table 2. Survey 1 parameters**

Start date	February 16, 1987
Stop date	February 24, 1987
Number of sweeps	232
Antenna orientation	zenith
Frequency range	1.0-10.4 GHz
Resolution	10 kHz
Time constant	$5 \times 10^{-4}$ sec
Baseline level	-133 dBm at 1 GHz, -126 dBm at 10 GHz
Threshold	10 dB above the baseline level

**Table 3. Frequencies with probability of interference ≥ 10 percent**

Center Frequency of RFI, MHz	Probability of RFI	RF Range Affected	Band Allocation <sup>a</sup>
1000.015	0.6	< 10 kHz wide	AN
1051.685	0.4	< 10 kHz wide	AN
1085.420	0.5	1085.4 MHz-1085.44 MHz	AN
1134.600	0.1	< 10 kHz wide	AN
1165.975	0.6	1165.94 MHz-1166.11 MHz	AN
1302.515	0.4	1302.5 MHz-1302.53 MHz	A
1310.850	1.0	< 10 kHz wide	AN
1723.410	0.2	< 10 kHz wide	F&M
1723.525	0.6	< 10 kHz wide	F&M
1723.640	0.2	< 10 kHz wide	F&M
1724.525	1.0	1724.5 MHz-1724.55 MHz	F&M
1905.020	0.6	< 10 kHz wide	F&M
2000.030	0.1	< 10 kHz wide	F&M
2110.850	0.1	< 10 kHz wide	AF&M
2112.420	0.2	< 10 kHz wide	F&M
2115.225	1.0	< 10 kHz wide	F&M
2605.020	0.5	< 10 kHz wide	BS
7786.785	0.9	7784.39 MHz-7789.18 MHz	F
7832.015	0.2	< 10 kHz wide	F
7879.970	0.5	7879.95 MHz-7879.99 MHz	F
7884.960	0.7	7884.93 MHz-7884.99 MHz	F
7889.970	0.3	7889.96 MHz-7889.98 MHz	F
7934.430	0.3	7934.15 MHz-7934.71 MHz	F&MS
7934.960	0.3	7934.89 MHz-7935.03 MHz	F&MS
7935.110	0.1	< 10 kHz wide	F&MS
7935.355	0.4	7935.25 MHz-7935.46 MHz	F&MS
7935.770	0.2	7935.69 MHz-7935.85 MHz	F&MS
8080.050	0.8	8079.73 MHz-8080.37 MHz	F&MS
8179.910	1.0	8179.88 MHz-8179.94 MHz	F&MS
8260.095	0.4	8260.06 MHz-8260.13 MHz	F&MS
8359.910	0.5	8359.89 MHz-8359.93 MHz	F&MS

<sup>a</sup>A = Aeronautical      AN = Aeronautical Navigation      BS = Broadcasting Satellite  
 F = Fixed              F&M = Fixed & Mobile              F&MS = Fixed & Mobile Satellite  
 (Partial listing from "Tables of Frequency Allocations and Other Extracts" from *Manual of Regulations and Procedures for Federal Radio Frequency Management*, Superintendent of Documents, Washington, D.C., January 1984.)

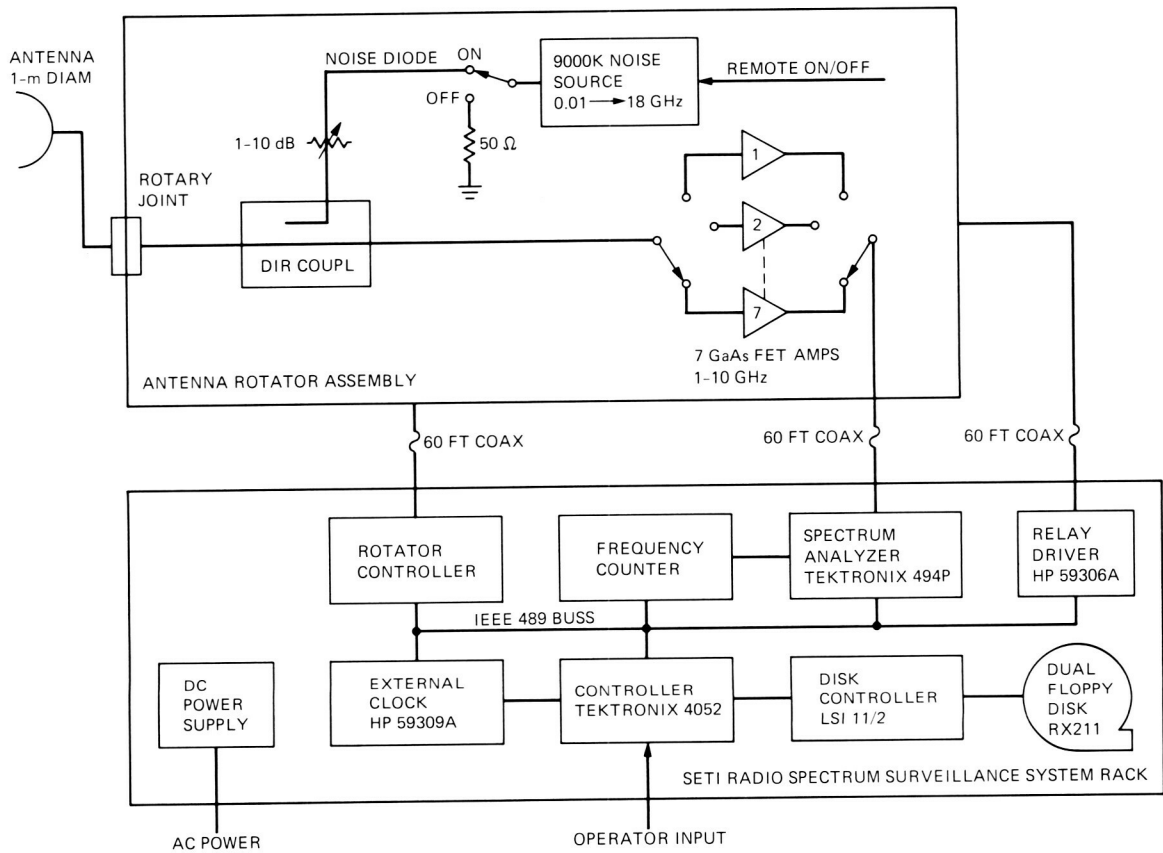


**Fig. 1. Radio Spectrum Surveillance System (RSSS) block diagram.**



**Fig. 2. Photograph of RSSS mounted on mobile van at Goldstone-Venus development station.**

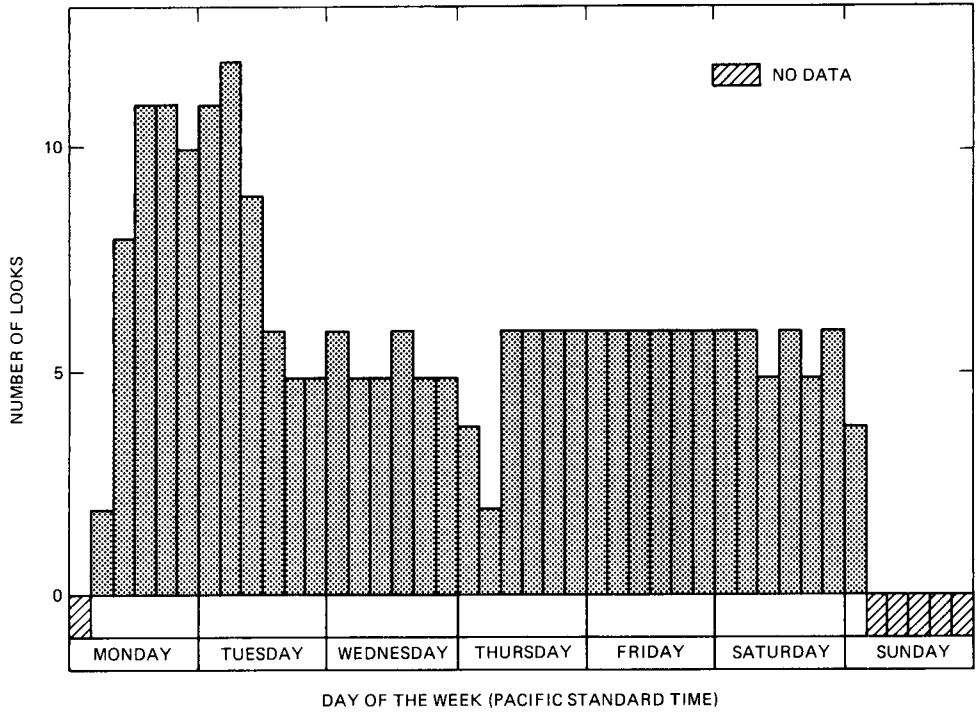


**Fig. 3. Number of looks versus day of week for Survey 1, 1.0–10.4 GHz.**

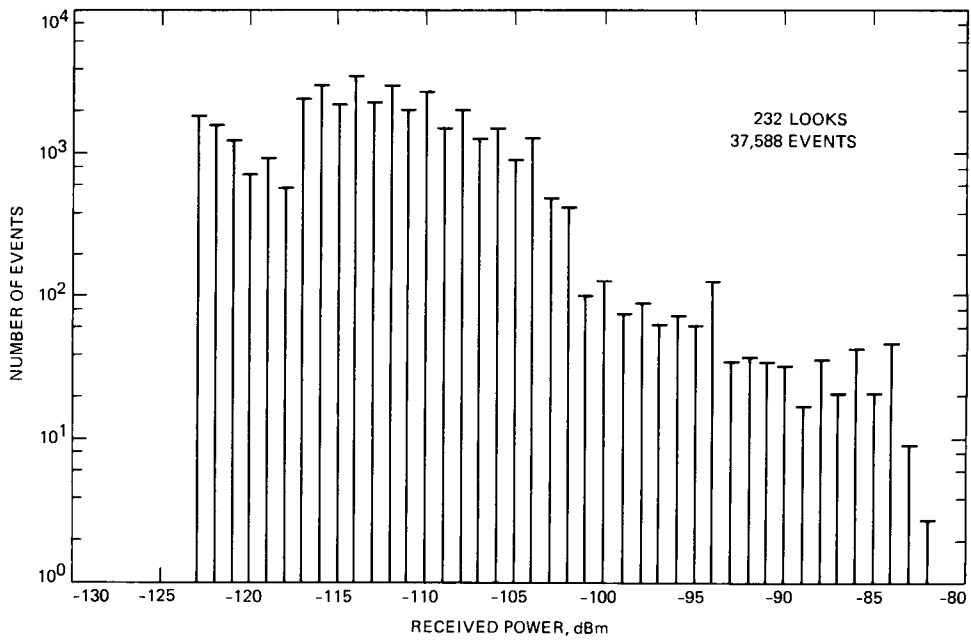


**Fig. 4. Histogram of number of RFI events as a function of received power for Survey 1, 1.0–10.4 GHz.**

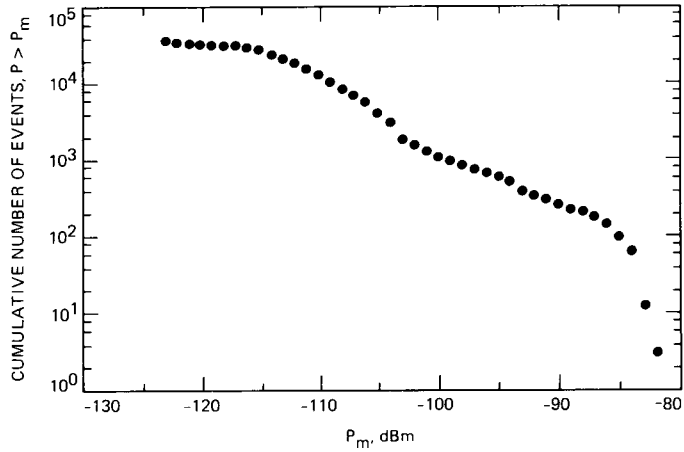


**Fig. 5. Cumulative histogram of number of RFI events as a function of  $P_m$  for Survey 1, 1.0–10.4 GHz.**

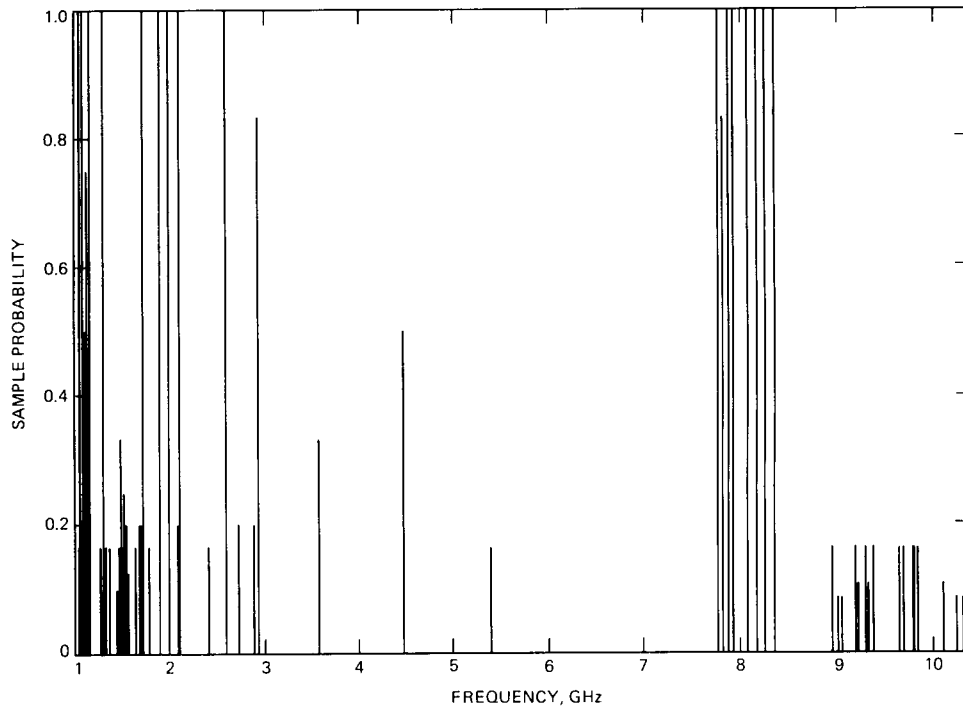


**Fig. 6. Probability of RFI events as a function of frequency for Survey 1, 1.0–10.4 GHz.**



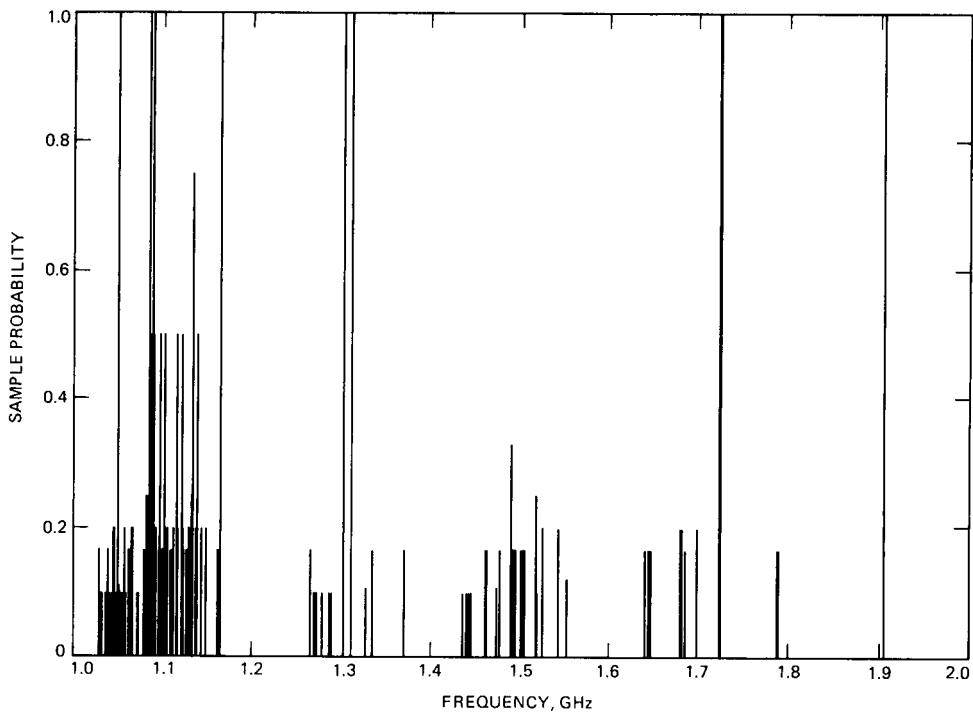


**Fig. 7. Probability of RFI events as a function of frequency for Survey 1, 1.0-2.0 GHz.**

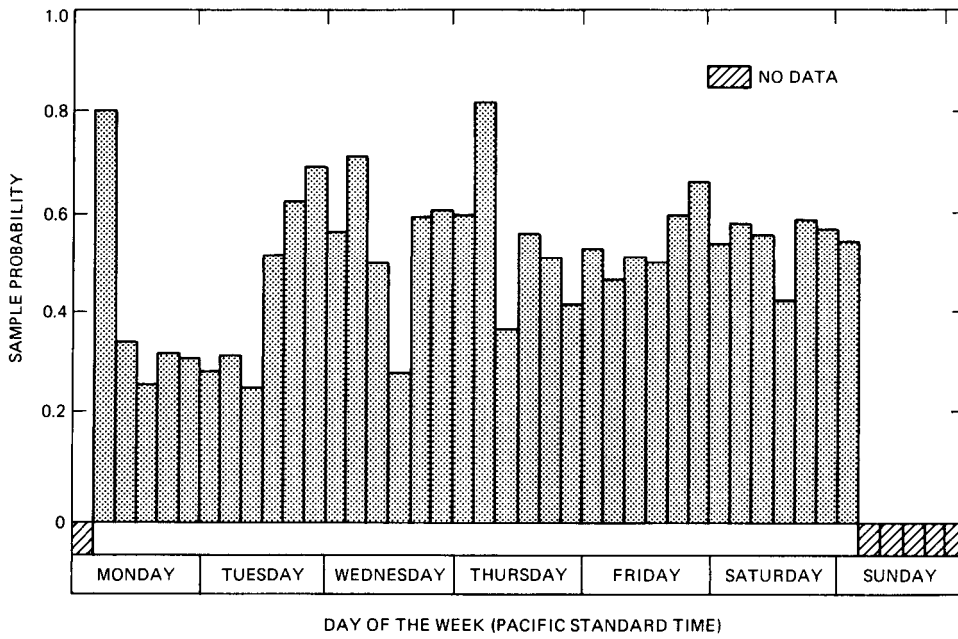


**Fig. 8. Probability of RFI events as a function of 4-hour slice of day of week for Survey 1, 1.0-10.4 GHz.**

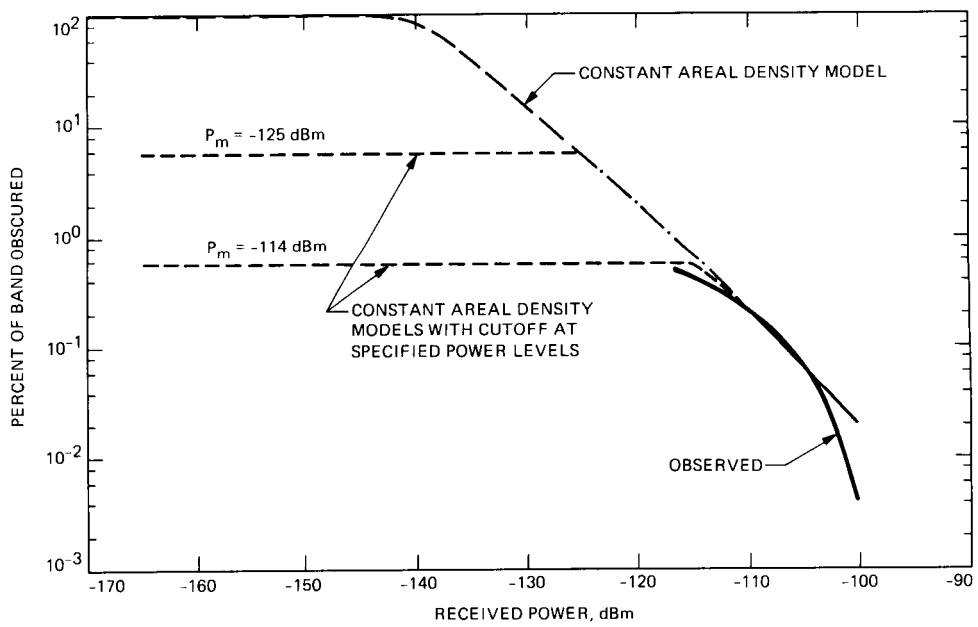


**Fig. 9. Observed and extrapolated percent of bandpass obscured by RFI events with probability greater than 10 percent, 1.0–10.4 GHz.**

## Errata

R. E. Hill (Ground Antenna and Facilities Engineering Section) has submitted the following errata to his article "A New State Space Model for the NASA/JPL 70-Meter Antenna Servo Controls" that appeared in the *Telecommunications and Data Acquisition Progress Report 42-91*, July-September 1987, November 15, 1987:

In Table 2 (page 253), the denominator,  $J_i$ , appearing in the equation for  $\dot{x}_2$  should be replaced with  $J_B$ . The variable,  $x_i$ , appearing in the equation for  $\dot{x}_{2i+4}$  should be replaced with  $x_1$ . The inequality symbol ( $\neq$ ) appearing in the equation for  $\dot{x}_{2i+4}$  should be replaced by a plus symbol (+).

In Table 3 (page 254), dashed lines are added to the linear system matrix to show the respective rows and columns corresponding to the flexible structure and alidade modes. The complexity of the changes to several elements of matrix  $\mathbf{F}$  necessitate the reproduction of the revised version in its entirety, below.

Also in Table 3 (page 255), the output vector  $H_{Ee}$  should appear:

$$H_{Ee} = [1 \ 0 \ 0 \ 0 \ \dots \ -1 \ 0 \ 0 \ 0 \ 0] \text{ Elevation only}$$

In the Notes section of Table 3 (page 255), the following errata were submitted:

Is	Should Be
$a_1 \dots a_5$	$a_1 \dots a_5$
$a_0$	$a_0$
$a_0 + a_1 + \dots + a_N = 1$	$a_0 + a_1 + \dots + a_N = 1$

Finally, in Table 4 (page 256), the term  $\frac{\omega_m^2}{v}$  should be  $\frac{\omega_m^2}{V}$ .

